

## Permittivity enhancement of aluminum oxide thin films with the addition of silver nanoparticles

R. Ravindran, K. Gangopadhyay, and S. Gangopadhyay<sup>a)</sup>

*Department of Electrical and Computer Engineering, University of Missouri, Columbia, Missouri 65211*

N. Mehta

*Texas Instruments, Dallas, Texas 75243*

N. Biswas

*Department of Electrical and Computer Engineering, North Carolina State University, Raleigh, North Carolina 27695*

(Received 29 March 2006; accepted 25 November 2006; published online 29 December 2006)

Multilayer reactive electron-beam evaporation of thin aluminum oxide layers with embedded silver nanoparticles (Ag-nps) has been used to create a dielectric thin film with an enhanced permittivity. The results show a frequency dependent increase of the dielectric constant  $\kappa$ . Overall stack  $\kappa$  of the control sample was found to be 7.7–7.4 in the 1 kHz–1 MHz range. This is in comparison with  $\kappa=16.7$ –13.0 over the same frequency range in the sample with Ag-nps. Capacitance-voltage and conductance-voltage measurements indicate the presence of charge capture resulting from the Ag-nps. The authors attribute this dielectric constant enhancement to dipole and space charge polarization mechanisms. © 2006 American Institute of Physics. [DOI: 10.1063/1.2425010]

Dielectric films with a large relative permittivity (high  $\kappa$ ) are of importance in a variety of applications ranging from complementary metal-oxide semiconductors (CMOSs) to dynamic memory devices. In the drive to find a replacement for SiO<sub>2</sub> in CMOS devices, oxides of hafnium and aluminum have emerged as leading candidates.<sup>1</sup> Robertson and Peacock have shown that aluminum oxide (Al<sub>2</sub>O<sub>3</sub>) has excellent conduction and valance band offsets on contact with Si.<sup>2,3</sup> This makes Al<sub>2</sub>O<sub>3</sub> ideally suited for use with *n*- and *p*-type Si over a range of doping levels. The drawback is that the intermediate dielectric constant of Al<sub>2</sub>O<sub>3</sub> limits the capacitance density compared with other high- $\kappa$  dielectrics. It is worth noting at this point that the permittivity of metal nanoparticles has been theorized to be superior to that predicted by the classical electrostatic model.<sup>4</sup> This is explained considering the dipole behavior of nonspherical nanoparticles dispersed in a medium. Each nanoparticle dipole is recognized as behaving like a basic harmonic oscillator or dipole with a relaxation frequency.<sup>5</sup>

The deposition of semiconductor device grade films of Al<sub>2</sub>O<sub>3</sub> and HfO<sub>2</sub> on Si is well established.<sup>6,7</sup> However, prior work on using noble metal nanoparticles to increase dielectric constants has focused primarily on polymer and glass dielectrics and processes that are not readily compatible with current integrated circuit fabrication.<sup>8–10</sup> Conversely, studies utilizing techniques similar to that used here have not focused explicitly on permittivity enhancement or dielectric properties.<sup>11</sup> The primary differences between the work presented here and earlier works on permittivity enhancement with nanoparticles are the manner in which the silver nanoparticles (Ag-nps) are deposited, the dielectric medium into which they dispersed, and the deposition and characterization of the film on Si substrates.

A control set without Ag-nps and an experimental set with Ag-nps were fabricated. In each set, samples were prepared on both *p*- and *p*<sup>+</sup>-Si (100) with resistivities of 1–10 and 0.0030–0.0070  $\Omega$  cm, respectively. The Si substrates were first cleaned with a modified Shiraki process to remove the native oxide and provide a clean, hydrogen passivated surface.<sup>12,13</sup> After drying under nitrogen, they were immediately transferred to a Kurt J. Lesker AXXIS e-beam evaporation system. From a base pressure of  $5 \times 10^{-7}$  torr, the substrates were heated to 50 °C and oxygen was introduced at 5 SCCM (SCCM denotes cubic centimeter per minute at STP) and  $5 \times 10^{-5}$  torr. For control samples without silver, 8.73 $\pm$ 0.08 nm of Al<sub>2</sub>O<sub>3</sub> was then evaporated at 0.5 Å/s. For samples with incorporated Ag-nps, Al<sub>2</sub>O<sub>3</sub>, approximately 3 nm in thickness, was deposited and the chamber was again pumped down to  $5 \times 10^{-7}$  torr. An ultrathin layer of Ag-nps, about half a nanometer in nominal thickness, was deposited under high vacuum. Oxygen was reintroduced, and approximately 3 nm of Al<sub>2</sub>O<sub>3</sub> was again evaporated. This process was repeated until the film consisted of three layers of Al<sub>2</sub>O<sub>3</sub> with two intermediate layers of Ag-nps. Similar to the control sample, the film was 9.60 $\pm$ 0.07 nm in total thickness. Thicknesses were measured using a Sigma Instruments crystal monitor during deposition and a J. A. Woolam variable angle ellipsometer after deposition. Measurements made using both methods were in agreement with each other. The samples were annealed, *in situ*, in a 45 SCCM,  $5 \times 10^{-4}$  torr hydrogen ambient at 250 °C for 45 min, after which a shadow mask was used to pattern titanium gates. Transmission electron microscope (TEM) images verified the presence of silver “nanoislands” or nanoparticles. Image analysis yielded a mean particle diameter of 2.0 $\pm$ 1.2 nm and a particle density of about 10<sup>12</sup> particles/cm<sup>2</sup> per silver layer. Banerjee and Chakravorty have shown that Ag-nps less than  $\approx$ 3 nm in diameter exhibit insulating properties.<sup>14</sup>

Device characterization consisted of capacitance-voltage (*C-V*) and conductance-voltage (*G-V*) measurements using an HP 4284A LCR meter and current-voltage (*I-V*) measure-

<sup>a)</sup> Author to whom correspondence should be addressed; electronic mail: gangopadhyays@missouri.edu

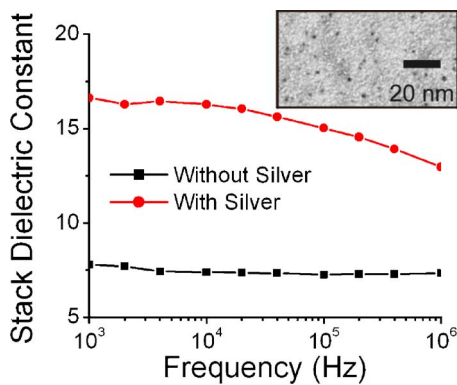


FIG. 1. (Color online) Dielectric constants of the two samples with and without silver. Inset is a top down TEM image showing one layer of silver nanoparticles on  $\text{Al}_2\text{O}_3$ .

ments using a Keithley 2400 sourcimeter. The  $p^+$ -Si:dielectric:Ti structure is discussed first. From an electrical standpoint, the  $p^+$ -Si behaves similar to a metal, and the device is thus a simple metal-insulator-metal capacitor. The dielectric constants are plotted in Fig. 1. As would be expected, the control sample exhibits relatively little frequency dependence on  $p^+$ -Si. However, the sample with embedded silver exhibits a frequency dependent enhancement of  $\kappa$ . Relative to the control sample, the Ag-np sample shows approximately a doubling in dielectric constant.

Two mechanisms are considered in explaining the frequency dependent nature of this permittivity increase. The first is space charge polarization at the Ag-np:dielectric interfaces. This is thought to apply more prominently to the particles above the conductor/insulator threshold for silver. Charge accumulation at the heterogeneous Ag-np:dielectric interface will produce an increase in capacitance most prominent at lower frequencies.<sup>15</sup> The Ag-nps are also proposed as behaving like induced dipoles with a frequency dependent response to the small signal. This has been observed in nanocomposite dielectrics with embedded metal nanoparticles.<sup>16,17</sup> As such, the second mechanism is a dipole polarization component. When the small signal frequency is sufficiently slower than the relaxation frequency of the Ag-nps, dipole polarization will contribute to the overall permittivity of the nanocomposite. The Ag-np dipole moments can follow the changes in an adequately low frequency small signal.<sup>5</sup> However, when the small signal frequency approaches the dipole relaxation frequency this ability decreases (typically occurring in the microwave region). We believe that dipole polarization is the primary permittivity enhancing mechanism in this nanocomposite system, particularly with regards to the smaller Ag-nps below the conduction threshold of silver. Between these two constituent mechanisms, the measured dielectric constant decreases with increasing frequencies. Considering space charge polarization, the dielectric constant drop at lower frequencies (around 1 kHz) is explained. Dipole polarization then ac-

TABLE I. Dissipation factors of the two samples over the tested frequency range.

Sample	1 kHz	10 kHz	100 kHz	1 MHz
Without silver	0.074	0.011	0.007	0.003
With silver	0.155	0.089	0.115	0.085

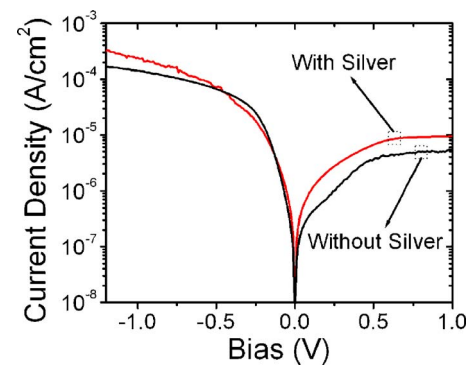


FIG. 2. (Color online) Current density curves for the control and experimental samples.

counts for the drop at higher frequencies (around 1 MHz). It is noted that both of these polarization mechanisms are lossy.

The dissipation factors  $D$  for the control and experimental samples over the measured frequency range are summarized in Table I. The increase in  $D$  in the Ag-np sample is attributed to the losses from charge accumulation at the Ag-np:dielectric interfaces (at lower frequencies) and alignment of the nanoparticle dipoles with the varying small signal (at higher frequencies).<sup>15</sup> Thus, there are some conceivable lower and upper frequencies (corresponding to the relaxation frequency), beyond which  $D$  should begin to decrease. Unfortunately, setup limitations prevented measurements outside of the reported frequency range.

Identical films forming metal-insulator-semiconductor (MIS) structures on  $p$ -Si were also characterized.  $I$ - $V$  measurements on the  $p$ -Si:dielectric:Ti structure are shown in Fig. 2. Leakage of both samples is roughly  $10^{-4}$  A/cm<sup>2</sup> in accumulation ( $V_{fb} - 0.5$  V =  $-0.70$  V with Ag and  $-1.25$  V without Ag), whereas the leakage of virtually identically processed 5 nm  $\text{HfO}_2$  is  $10^{-2}$  A/cm<sup>2</sup>.<sup>6</sup> This indicates that the addition of silver does not make the dielectric notably leakier and is in line with similarly fabricated high- $\kappa$  thin films.

All MIS data were corrected for the presence of series resistance  $R_s$ .<sup>18</sup> Since the Ag-nps themselves are close to each other but not at the interface and because of the low temperature processing, they are not expected to affect the interface states. However, the Ag-nps establish locations of quantum confinement (QC) within the nanocomposite dielectric. Because of the close proximity of the first and second

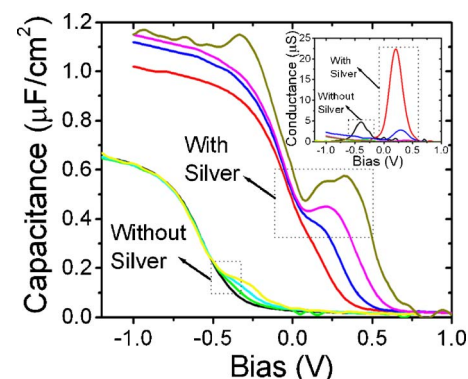


FIG. 3. (Color online) Capacitance-voltage (top) and measured conductance-voltage (inset) curves on  $p$ -Si. The group of four curves on the left is from the control sample, and the group of four curves on the right is from the experimental sample. Within each group, frequencies left to right are 1 MHz, 100 kHz, 10 kHz, and 1 kHz.

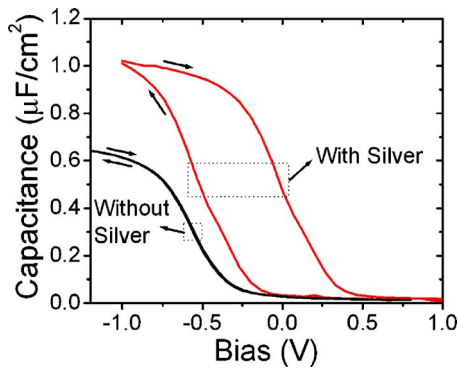


FIG. 4. (Color online) High frequency (1 MHz) capacitance-voltage hysteresis curves on *p*-Si for both samples.

Ag-np layers with the Si substrate and gate interfaces, respectively, resonant tunneling to and from the QC sites is possible.<sup>19</sup> That is, as the Fermi level crosses a discrete Ag-np energy level, carriers can tunnel through the first Al<sub>2</sub>O<sub>3</sub> layer and onto the Ag-nps within the oxide. Charge loading and unloading onto the Ag-nps is measured as an increased conductance in the Ag-np sample, as shown in Fig. 3 (*G-V* curves).<sup>20</sup> This is additionally supported by the observed “hump” in the low frequency *C-V* curves of Fig. 3, which is the result of resonant tunneling events involving Ag-nps. Others have observed similar behavior in Si nanoparticles embedded in SiO<sub>2</sub>.<sup>21</sup> Further validating this concept, there is a memory effect, as shown in Fig. 4. A hysteresis window of approximately 0.5 V is present in the Ag-np sample, whereas virtually none is present in the control sample. Using this hysteresis ( $\Delta=0.5$  V) and  $N_t=C_{ox}\Delta/q$ , the charge density  $N_t$  is found to be  $3.18 \times 10^{12}$  charges/cm<sup>2</sup>. The device thus behaves as a floating gate memory device utilizing the nanoparticles as charge storage locations.<sup>11,22</sup>

In summary, our work has shown that Al<sub>2</sub>O<sub>3</sub> films embedded with Ag-nps have increased permittivity. With the addition of Ag-nps, the dielectric constant was approximately doubled in a frequency dependent manner relative to a control sample without Ag-nps. Also, the introduction of Ag-nps established QC sites within the dielectric near the

gate and Si interfaces to which carriers could be loaded and unloaded via resonant tunneling, as evidenced by the *C-V* and *G-V* curves.

The authors thank M. Othman for ellipsometry measurements. They are also grateful for the funding provided by the National Science Foundation Grant No. ECS0223.

<sup>1</sup>G. D. Wilk, R. M. Wallace, and J. M. Anthony, *J. Appl. Phys.* **89**, 5243 (2001).

<sup>2</sup>John Robertson, *J. Vac. Sci. Technol. B* **18**, 1785 (2000).

<sup>3</sup>P. W. Peacock and J. Robertson, *J. Appl. Phys.* **92**, 4712 (2002).

<sup>4</sup>P. Gor'kov and G. M. Eliashberg, *Sov. Phys. JETP* **21**, 940 (1965).

<sup>5</sup>T. Kempa, D. Carnahan, M. Olek, M. Correa, M. Giersig, M. Cross, G. Benham, M. Sennett, Z. Ren, and K. Kempa, *J. Appl. Phys.* **98**, 034310 (2005).

<sup>6</sup>H. Harris, K. Choi, N. Mehta, A. Chandolu, N. Biswas, G. Kipshidze, S. Nikishin, S. Gangopadhyay, and H. Temkin, *Appl. Phys. Lett.* **81**, 1065 (2002).

<sup>7</sup>E. P. Gusev, M. Copel, E. Cartier, I. J. R. Baumvol, C. Krug, and M. A. Gribelyuk, *Appl. Phys. Lett.* **76**, 176 (2000).

<sup>8</sup>T. K. Kundu and D. Chakravorty, *Appl. Phys. Lett.* **67**, 2732 (1995).

<sup>9</sup>P. K. Mukherjee and D. Chakravorty, *J. Mater. Res.* **17**, 3127 (2002).

<sup>10</sup>S. K. Saha, *Phys. Rev. B* **69**, 125416 (2004).

<sup>11</sup>Ch. Sargentis, K. Giannakopoulos, A. Travlos, N. Boukus, and D. Tsamakis, *Appl. Phys. Lett.* **88**, 073106 (2006).

<sup>12</sup>A. Ishizaka and Y. Shiraki, *J. Electrochem. Soc.* **133**, 666 (1986).

<sup>13</sup>K. Choi, H. Harris, S. Gangopadhyay, and H. Temkin, *J. Vac. Sci. Technol. A* **21**, 718 (2003).

<sup>14</sup>S. Banerjee and D. Chakravorty, *Appl. Phys. Lett.* **72**, 1027 (1998).

<sup>15</sup>Arthur R. Von Hippel, *Dielectric Materials and Applications* (Technology Press of MIT, Massachusetts, 1995), pp. 18–39

<sup>16</sup>Jianwen Xu and C. P. Wong, *Proceedings of the Ninth International Symposium on Advanced Packaging Materials: Processes, Properties and Interfaces* (IEEE, New York, 2004) pp. 158–170.

<sup>17</sup>G. C. Vezzoli, M. F. Chen, and J. Caslavsky, *Ceram. Int.* **23**, 105 (1997).

<sup>18</sup>E. H. Nicollian and J. R. Brews, *MOS (Metal Oxide Semiconductor) Physics and Technology* (Wiley, New Jersey, 2003), pp. 222–224.

<sup>19</sup>L. W. Yu, K. J. Chen, L. C. Wu, M. Dai, W. Li, and X. F. Huang, *Phys. Rev. B* **71**, 245305 (2005).

<sup>20</sup>T. H. Ng, W. K. Chim, and W. K. Choi, *Appl. Phys. Lett.* **88**, 113112 (2006).

<sup>21</sup>Jianjun Shi, Liangcai Wu, Xinfan Huang, Jiayu Liu, Zhongyuan Ma, Wei Li, Xuefei Li, Jun Xu, Di Wu, Aidong Li, and Kunji Chen, *Solid State Commun.* **123**, 437 (2002).

<sup>22</sup>Shaoyun Huang, Sourii Banerjee, and Shunri Oda, *Mater. Res. Soc. Symp. Proc.* **686**, A8.8.1 (2002).